

# Standard enthalpies of formation of scandium alloys, Sc+Me (Me≡Fe, Co, Ni, Ru, Rh, Pd, Ir, Pt), by high-temperature calorimetry

N. Selhaoui and O. J. Kleppa

James Franck Institute, University of Chicago, 5640 S. Ellis Avenue, Chicago, IL 60637 (USA)

(Received September 1, 1992)

## Abstract

The standard enthalpies of formation of scandium alloys, Sc+Me (Me≡Fe, Co, Ni, Ru, Rh, Pd, Ir, Pt) were determined by direct synthesis calorimetry at  $1473 \pm 2$  K. The following values of  $\Delta_f H_m^\circ$  (kJ g atom<sup>-1</sup>) are reported: Fe<sub>2</sub>Sc,  $-(11.2 \pm 1.2)$ ; Co<sub>2</sub>Sc,  $-(32.5 \pm 2.1)$ ; CoSc<sub>2</sub>,  $-(26.7 \pm 1.9)$ ; Ni<sub>2</sub>Sc,  $-(43.0 \pm 2.3)$ ; NiSc,  $-(44.7 \pm 2.3)$ ; RuSc,  $-(44.5 \pm 2.2)$ ; Rh<sub>3</sub>Sc,  $-(51.7 \pm 1.4)$ ; RhSc,  $-(94.5 \pm 1.5)$ ; PdSc,  $-(89.3 \pm 2.2)$ ; IrSc,  $-(89.7 \pm 3.0)$ ; Ir<sub>2</sub>Sc,  $-(66.3 \pm 1.3)$ ; PtSc,  $-(104.8 \pm 5.4)$ . The results are compared with predicted values, and with earlier data for some of the corresponding yttrium and titanium alloys.

## 1. Introduction

In the past decade there has been greatly increased interest in the thermodynamics of alloys. During recent years, we have pursued systematic studies of the thermochemistry of intermetallic compounds formed between early transition metals and late transition metals. In these investigations, we have applied two different calorimetric methods: direct synthesis calorimetry, used in our recent study of yttrium alloys [1], and solute-solvent drop calorimetry adopted in our studies of alloys of Ti, Zr and Hf with the platinum group metals [2]. In the present communication these studies are extended to the alloys of the Group III metal scandium with the iron and platinum group metals. In the course of the present investigations, we have measured the standard enthalpies of formation of 12 intermetallic phases in eight binary systems by direct synthesis calorimetry. Our results are compared with thermochemical data in the published literature and with available values for alloys of titanium and yttrium with the same metals. Our results are also compared with predicted values from Miedema's semi-empirical model [3] and from Watson and Bennett's model [4].

## 2. Experimental details

### 2.1. General

Some of the equilibrium phase diagrams for the binary alloys considered are not available, notably the

diagrams for the Sc+Ir and Sc+Rh systems. However, the other phase diagrams [5, 6] show that the intermetallic compounds in the systems considered (with one exception, CoSc<sub>2</sub>, which melts near 1113 K) all have fairly high melting temperatures which range from 1600 K to 2500 K. Since we expected strong chemical interaction between the metals, we decided to measure their enthalpies of formation by direct synthesis of the compounds from the elements. In this approach, powders of the two components are mixed together in the appropriate proportions, compressed into small cylindrical pellets, and then dropped into the high-temperature calorimeter where they react chemically.

The calorimetric experiments were carried out at  $1473 \pm 2$  K in a single-unit differential calorimeter that is described in some detail elsewhere [7]. This calorimeter is based on the same principle as the commercial Setaram unit, but is maintained continuously at high temperature by a Pt-40%Rh heating element rather than heated intermittently by a graphite resistor. In this calorimeter, the temperature record of the reacting system is measured by means of a multiple-junction axial thermopile. The reaction chamber of the calorimeter consists of a thin-walled 20 mm outside diameter, 10 cm long BN crucible that protects the Pt-20%Rh "liner" from the contents of a small 15 mm diameter BeO crucible in which the reaction actually takes place. All experiments were carried out in an atmosphere of argon gas that was purified by passing the gas over titanium powder at about 1173 K.

Calibration of the calorimeter was achieved by dropping small pieces of 3 mm diameter, high purity, copper rod from room temperature into the calorimeter cell. Within a single series of measurements, the calibrations were reproducible within  $\pm 1.5\%$ . The molar enthalpy of pure copper at 1473 K ( $46465 \text{ J mol}^{-1}$ ) was taken from Hultgren *et al.* [8].

## 2.2. Materials

The metallic purities of the metals and the sizes of the powders used in the present experiments are summarized in Table 1. With the exception of the scandium metal, the impurity levels are negligible compared with our experimental errors.

The scandium powder was prepared from the lump metal by filing and then sifting the powder through an 80-mesh sieve. X-ray diffraction and scanning electron microscopy (SEM) of this powder showed a small amount of Ta estimated at about 2 at.%. We believe that the Ta metal remains essentially inert in the chemical reactions considered. We made a correction for the Ta content in weighing out the scandium powder. The iron, cobalt and nickel powders were used after reduction for 1 h in a flow of  $\text{H}_2$  gas near 900 K. All the metals used, except the rhodium powder, were purchased from Johnson-Matthey, AESAR Group. The rhodium metal was purchased from Engelhard.

## 3. Results

In the direct combination method, the standard enthalpies of formation of the intermetallic compounds are obtained from the heat effects associated with two consecutive calorimetric experiments:

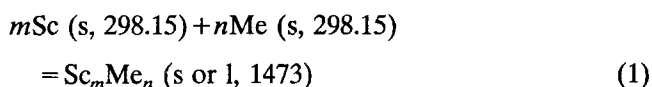


TABLE 1. Metallic purity and description of the materials used in the calorimetric measurements

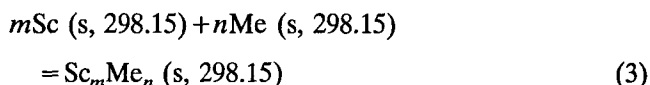
| Metal | Metallic purity (%) | Comments                              |
|-------|---------------------|---------------------------------------|
| Sc    | 99.99 <sup>a</sup>  | Lump, sublimed dendritic <sup>a</sup> |
| Fe    | 99.9                | –325 mesh powder                      |
| Co    | 99.8                | –300 mesh powder                      |
| Ni    | 99.9                | –400 mesh powder                      |
| Ru    | 99.9                | –100 mesh powder                      |
| Rh    | 99.9                | –100 mesh powder                      |
| Pd    | 99.95               | –200 mesh powder                      |
| Ir    | 99.95               | –150 mesh powder                      |
| Pt    | 99.99               | –325 mesh powder                      |

<sup>a</sup>X-ray diffraction and SEM examination of the filed powder prepared from this sample showed an amount of Ta estimated at about 2 at.%.

and



where Me in the present study represents Fe, Co, Ni, Ru, Rh, Pd, Ir and Pt, and s and l denote solid and liquid respectively. Among the compounds studied in the present investigation, only  $\text{CoSc}_2$  was liquid at 1473 K. From eqns. (1) and (2) we get:



The standard enthalpy of formation,  $\Delta_f H_m^\circ$ , is obtained from the molar enthalpy changes associated with eqns. (1) and (2):

$$\Delta_f H_m^\circ (\text{Sc}_m\text{Me}_n) = \Delta H_m (1) - \Delta H_m (2) \quad (4)$$

A summary of all the experimental results obtained in the course of the present investigation is given in Table 2. The reported values of  $\Delta H_m (1)$  and  $\Delta H_m (2)$  are averages of four to six experiments with standard deviations  $\delta_1$  and  $\delta_2$ . The uncertainty in  $\Delta_f H_m^\circ$  was calculated from  $\delta = (\delta_1^2 + \delta_2^2)^{1/2}$ . After the experiments, all alloy samples were examined by powder X-ray diffraction and by SEM and energy dispersive X-ray micro-analysis. The results of our X-ray diffraction and SEM for all the compounds considered are summarized in Table 3. The X-ray diffraction pattern for  $\text{PtSc}$  was, in the main, similar to the one published by Aldred [9], *i.e.* the  $\text{CsCl}$  type structure; while other lines remained unindexed, the SEM of the sample showed a single phase.

## 4. Discussion

To the best of our knowledge, the only experimental enthalpy of formation value for the systems considered in the published literature is the calorimetric value for  $\text{PdSc}$  of Gachon *et al.* [10]. Their value,  $-106 \text{ kJ g atom}^{-1}$ , is significantly more exothermic than ours,  $-89 \text{ kJ g atom}^{-1}$ . However, Gachon's value was reported as "indicative" with an estimated uncertainty in the range  $\pm 15 \text{ kJ g atom}^{-1}$ .

Figure 1 shows a plot of our experimental results for  $\text{Sc} + \text{Fe}$ ,  $\text{Sc} + \text{Co}$  and  $\text{Sc} + \text{Ni}$ ; Fig. 2 gives our values for  $\text{Sc} + \text{Ru}$ ,  $\text{Sc} + \text{Rh}$  and  $\text{Sc} + \text{Pd}$ ; and Fig. 3 shows the results for  $\text{Sc} + \text{Ir}$  and  $\text{Sc} + \text{Pt}$ . All values in these figures are given in  $\text{kJ g atom}^{-1}$ .

For all the alloys studied in this investigation, predicted values of the enthalpies of formation are available from the semi-empirical theory of de Boer *et al.* [3] and for the equiatomic alloys also from Watson and Bennett [4]. For the  $\text{Rh} + \text{Sc}$  and  $\text{Ir} + \text{Sc}$  systems, there

TABLE 2. Observed heats of reaction, average heat contents at 1473 K, and calculated standard enthalpies of formation, in kJ g<sup>-1</sup> atom<sup>-1</sup> <sup>a</sup>

| Compound                              | $\Delta H_{\text{obs}} = \Delta H_m(1)$ | $H_{1473}^\circ - H_{298.15}^\circ = \Delta H_m(2)$ | $\Delta_f H_m^\circ$ |
|---------------------------------------|---|---|----------------------|
| Fe <sub>2</sub> Sc                    | 27.45 ± 1.04 (6)                        | 38.68 ± 0.56 (5)                                    | -11.2 ± 1.2          |
| Co <sub>2</sub> Sc                    | 4.47 ± 1.02 (5)                         | 36.92 ± 1.86 (5)                                    | -32.5 ± 2.1          |
| CoSc <sub>2</sub>                     | 22.70 ± 0.61 (5)                        | 49.41 ± 1.79 (5)                                    | -26.7 ± 1.9          |
| Ni <sub>2</sub> Sc                    | -3.32 ± 0.74 (5)                        | 39.63 ± 2.22 (5)                                    | -43.0 ± 2.3          |
| NiSc                                  | -10.68 ± 1.39 (5)                       | 34.04 ± 1.79 (5)                                    | -44.7 ± 2.3          |
| RuSc                                  | -10.53 ± 2.00 (6)                       | 33.98 ± 0.84 (5)                                    | -44.5 ± 2.2          |
| Rh <sub>3</sub> Sc                    | -19.30 ± 1.05 (6)                       | 32.36 ± 0.92 (5)                                    | -51.7 ± 1.4          |
| RhSc                                  | -61.24 ± 1.04 (6)                       | 33.22 ± 1.04 (5)                                    | -94.5 ± 1.5          |
| PdSc                                  | -53.21 ± 0.95 (6)                       | 36.12 ± 1.96 (4)                                    | -89.3 ± 2.2          |
| IrSc                                  | -59.21 ± 1.82 (5)                       | 30.50 ± 2.31 (4)                                    | -89.7 ± 3.0          |
| Ir <sub>2</sub> Sc                    | -33.34 ± 1.22 (6)                       | 32.91 ± 0.56 (4)                                    | -66.3 ± 1.3          |
| Ir <sub>0.48</sub> Sc <sub>0.52</sub> | -59.47 ± 1.17 (5)                       | 30.67 ± 0.47 (5)                                    | -90.1 ± 1.3          |
| Ir <sub>0.4</sub> Sc <sub>0.6</sub>   | -50.41 ± 2.03 (5)                       | 31.54 ± 1.75 (4)                                    | -82.0 ± 2.7          |
| PtSc                                  | -73.41 ± 5.23 (5)                       | 31.36 ± 1.48 (5)                                    | -104.8 ± 5.4         |

<sup>a</sup>Numbers in parentheses indicate number of experiments averaged.

TABLE 3. Summary of X-ray diffraction and SEM examination

| Compound                              | X-ray diffraction examination |  | SEM examination                                      |
|---------------------------------------|-------------------------------|--|--|
|                                       | Literature structure          | Found structure  |  |
| Fe <sub>2</sub> Sc                    | MgZn <sub>2</sub>             | MgZn <sub>2</sub> + other phases (<5 at.%)                   | Fe <sub>2</sub> Sc abundant + other phases (<5 at.%) |
| Co <sub>2</sub> Sc                    | MgCu <sub>2</sub>             | MgCu <sub>2</sub> + Sc <sub>2</sub> O <sub>3</sub> (<5 at.%) | Co <sub>2</sub> Sc single phase                      |
| CoSc <sub>2</sub>                     | CuAl <sub>2</sub>             | CuAl <sub>2</sub> + other phases (<5 at.%)                   | CoSc <sub>2</sub> abundant + other phases (<5 at.%)  |
| Ni <sub>2</sub> Sc                    | Ti <sub>2</sub> Ni            | Ti <sub>2</sub> Ni + NiSc phase (<5 at.%)                    | Ni <sub>2</sub> Sc abundant + NiSc phase (<5 at.%)   |
| NiSc                                  | CsCl                          | CsCl + second phase (<5 at.%)                                | NiSc single phase                                    |
| RuSc                                  | CsCl                          | CsCl + Ru (<5 at.%)  | RuSc abundant + Ru (<5 at.%)                         |
| RhSc                                  | CsCl                          | CsCl   | RhSc single phase                                    |
| Rh <sub>3</sub> Sc                    | AuCu <sub>3</sub>             | AuCu <sub>3</sub>  | Rh <sub>3</sub> Sc abundant + RhSc (<5 at.%)         |
| PdSc                                  | CsCl                          | CsCl   | PdSc single phase                                    |
| IrSc                                  | CsCl                          | CsCl + Ir <sub>2</sub> Sc (<5 at.%)                          | IrSc abundant + other phase (<10 at.%)               |
| Ir <sub>2</sub> Sc                    | MgCu <sub>2</sub>             | MgCu <sub>2</sub> + IrSc (<5 at.%)                           | Ir <sub>2</sub> Sc abundant + other phase (<10 at.%) |
| Ir <sub>0.48</sub> Sc <sub>0.52</sub> | —                             | CsCl + Ir <sub>2</sub> Sc (<5 at.%)                          | IrSc abundant + other phase (<10 at.%)               |
| Ir <sub>0.4</sub> Sc <sub>0.6</sub>   | —                             | CsCl + unknown phase   | IrSc + unknown phase                                 |
| PtSc                                  | CsCl                          | See "Results"  | PtSc single phase                                    |

is fairly good agreement between our experiments and de Boer *et al.*, but for the other systems this theory predicts more exothermic values than observed (see Figs. 1–3). From these figures, we also see that the

model of Watson and Bennett usually predicts too exothermic values. However, for PdSc their value of -98 kJ g atom<sup>-1</sup> is fairly close to our experimental result.

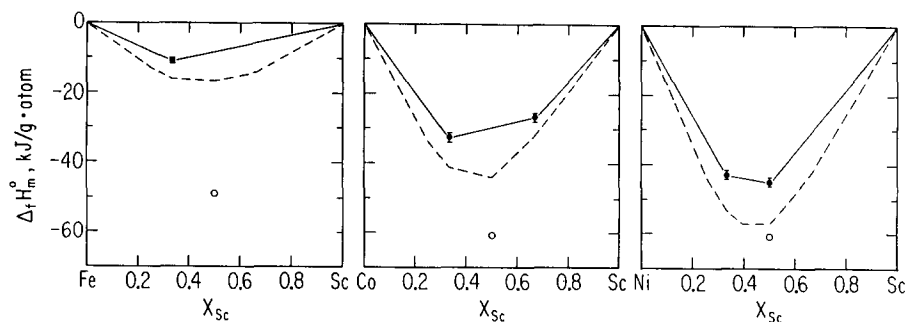


Fig. 1. Standard enthalpies of formation for alloys of Sc with Fe, Co and Ni, compared with predicted values of de Boer *et al.* [3] and of Watson and Bennett [4].  $\blacksquare$  = present work, --- = de Boer *et al.*,  $\circ$  = Watson and Bennett.

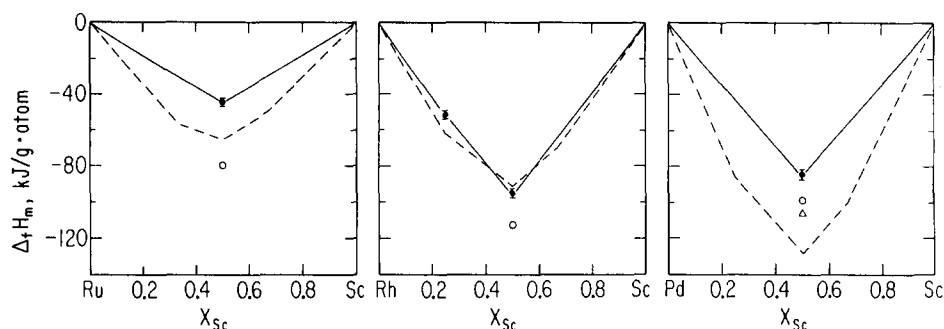


Fig. 2. Standard enthalpies of formation for alloys of Sc with Ru, Rh and Pd, compared with predicted values of de Boer *et al.* [3] and of Watson and Bennett [4].  $\blacksquare$  = present work, --- = de Boer *et al.*,  $\circ$  = Watson and Bennett,  $\triangle$  = Gachon *et al.*

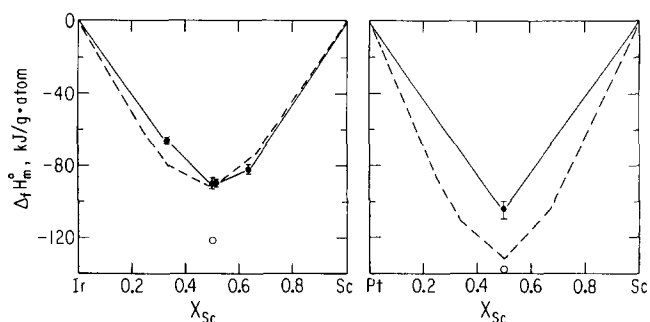


Fig. 3. Standard enthalpies of formation for alloys of Sc with Ir and Pt, compared with predicted values of de Boer *et al.* [3] and of Watson and Bennett [4].  $\blacksquare$  = present work, --- = de Boer *et al.*,  $\circ$  = Watson and Bennett.

In Figs. 4–6 we compare our results for the scandium alloys with corresponding data for alloys of titanium and yttrium. We note first in Fig. 4 that the standard enthalpies of formation of the Ni+Sc alloys are more exothermic than the corresponding alloys of Ni+Ti [11] and of Ni+Y [12, 13]. For  $\text{Co}_2\text{Sc}$  and  $\text{Fe}_2\text{Sc}$  the values of the standard enthalpies of formation are intermediate between the corresponding values for  $\text{Co}_2\text{Ti}$  [14, 15] and  $\text{Co}_2\text{Y}$  [16] and between  $\text{Fe}_2\text{Ti}$  [14, 15] and  $\text{Fe}_2\text{Y}$  [17].

We note next in Fig. 5 that the value for  $\text{PdSc}$ ,  $-89 \text{ kJ g atom}^{-1}$ , is close to the value for  $\text{PdY}$ ,  $-95 \text{ kJ g atom}^{-1}$  (1), while the value for  $\text{PdTi}$ ,  $-52 \text{ kJ g atom}^{-1}$

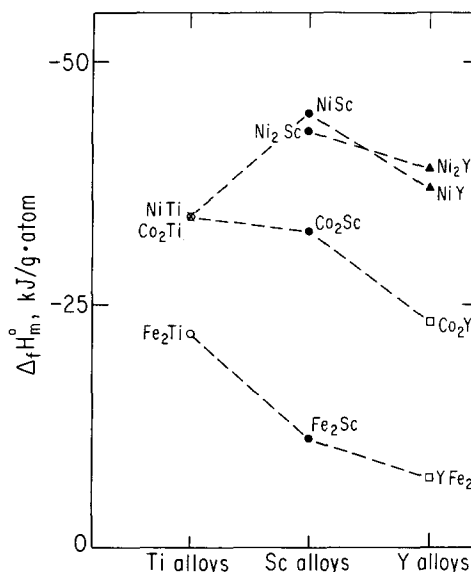


Fig. 4. Comparison of enthalpies of formation for alloys of Sc with Fe, Co and Ni, with corresponding data for alloys of Ti and Y.  $\bullet$  = present work,  $\circ$  = Gachon *et al.*,  $\times$  = Gomozov *et al.*,  $\square$  = Subramanian and Smith,  $\blacktriangle$  = Colinet *et al.*

(2), is much less exothermic. Note also that the value for  $\text{RhSc}$ ,  $-94.5 \text{ kJ g atom}^{-1}$ , is more exothermic than the corresponding alloys  $\text{RhY}$ ,  $-76 \text{ kJ g atom}^{-1}$  (1), and  $\text{RhTi}$ ,  $-72 \text{ kJ g atom}^{-1}$  (2). The value for  $\text{RuSc}$ ,  $-44.5 \text{ kJ g atom}^{-1}$ , is much more exothermic than the

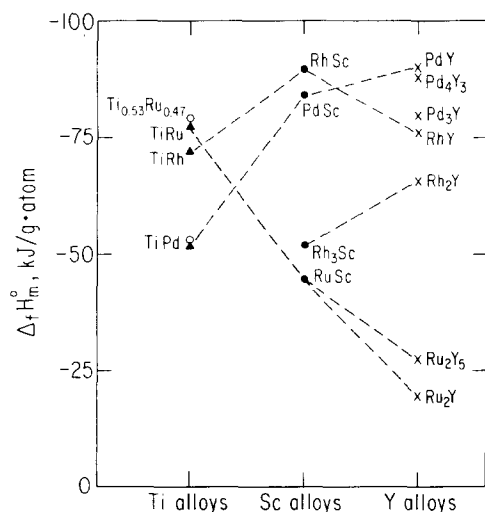


Fig. 5. Comparison of enthalpies of formation for alloys of Sc with Ru, Rh and Pd, with corresponding data for alloys of Ti and Y. ● = present work, ▲ = Topor and Kleppa, ○ = Gachon *et al.*, × = Selhaoui and Kleppa.

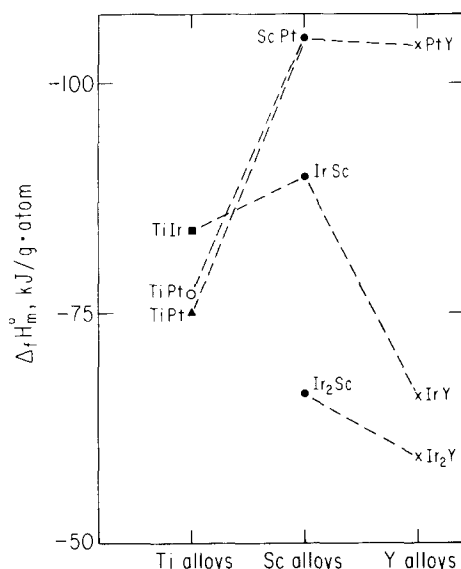


Fig. 6. Comparison of enthalpies of formation for alloys of Sc with Ir and Pt, with corresponding data for alloys of Ti and Y. ● = present work, × = Selhaoui and Kleppa, ○ = Selhaoui and Gachon, ▲ = Topor and Kleppa, ■ = Gachon *et al.*

Ru + Y alloys (1), but less exothermic than TiRu,  $-77$  kJ g atom $^{-1}$  (2). In Fig. 6 we see that our value for ScPt,  $-105$  kJ g atom $^{-1}$ , is very similar to the value

for PtY,  $-104$  kJ g atom $^{-1}$  (1), while the value for PtTi is much less exothermic,  $-75$  kJ g atom $^{-1}$  (2). The standard enthalpy of formation of IrSc,  $-90$  kJ g atom $^{-1}$ , is fairly close to the value for TiIr,  $-84$  kJ g atom $^{-1}$  (2), while the value for IrY,  $-66$  kJ g atom $^{-1}$  (1) is significantly less exothermic.

## Acknowledgments

This work has been supported by NSF under grant CHE-9014789 and has also benefited from the general facilities of the University of Chicago MRL. We are indebted to Dr. A. M. Davis who carried out the SEM and energy dispersive X-ray analyses.

## References

- 1 N. Selhaoui and O. J. Kleppa, *J. de Chimie Physique*, submitted for publication.
- 2 L. Topor and O. J. Kleppa, *J. Less Common Metals*, 155 (1989) 61, and references therein.
- 3 F. R. de Boer, R. Boom, W. C. M. Mattens, A. R. Miedema and A. K. Niessen, *Cohesion in Metals, Transition Metal Alloys*, North-Holland, Amsterdam, 1988.
- 4 R. E. Watson and L. H. Bennett, *Calphad*, 8 (1984) 307.
- 5 W. G. Moffat, *The Handbook of Binary Phase Diagrams*, Genium, Schenectady, NY, 1984.
- 6 T. B. Massalski (ed.), *Binary Alloy Phase Diagrams*, 2nd edition, ASM International, Materials Park, Ohio, 1990.
- 7 O. J. Kleppa and L. Topor, *Thermochim. Acta*, 139 (1989) 291.
- 8 R. Hultgren, P. D. Desai, D. T. Hawkins, M. Gleiser, K. K. Kelley and D. D. Wagman, *Selected Values of Thermodynamic Properties of the Elements*, ASM, Metals Park, Ohio, 1973.
- 9 A. T. Aldred, *Trans. A.I.M.E.*, 224 (1962) 1082.
- 10 J. C. Gachon, J. Charles and J. Hertz, *Calphad*, 9 (1985) 29.
- 11 P. A. Gomofov, Yu. V. Zasypalov and B. M. Mogutnov, *Russ. J. Phys. Chem.*, 60 (1986) 1122.
- 12 C. Colinet, A. Pasturel and K. H. J. Buschow, *J. Appl. Phys.*, 62 (1987) 3712.
- 13 C. Colinet, A. Pasturel and K. H. J. Buschow, in *Proc. Conf. on Liquid and Amorphous Metals*, Garmish-Partenkirchen, 1986, p. 277.
- 14 J. C. Gachon, M. Notin and J. Hertz, *Thermochim. Acta*, 48 (1981) 155.
- 15 J. C. Gachon and J. Hertz, *Calphad*, 7 (1983) 1.
- 16 P. R. Subramanian and J. F. Smith, *Metall. Trans.*, 16B (1985) 577.
- 17 P. R. Subramanian and J. F. Smith, *Calphad*, 8 (1984) 295.